arXiv:1604.08829v1 [cond-mat.quant-gas] 29 Apr 2016

Engineering interactions and anyon statistics by multicolor lattice-depth modulations

Lorenzo Cardarelli,[1] Sebastian Greschner,[1] and Luis Santos[1]

[1] *Institut für Theoretische Physik, Leibniz Universität Hannover, Appelstr. 2, DE-30167 Hannover, Germany*

(Dated: May 2, 2016)

We show that a multicolor modulation of the depth of an optical lattice allows for a flexible independent control of correlated hopping, occupation-dependent gauge fields, effective on-site interactions without Feshbach resonances, and nearest-neighbor interactions. As a result, the lattice-depth modulation opens the possibility of engineering with minimal experimental complexity a broad class of lattice models in current experiments with ultra-cold atoms, including Hubbard models with correlated hopping, peculiar extended models, and two-component anyon-Hubbard models.

PACS numbers: 37.10.Jk, 67.85.-d, 05.30.Pr

Floquet engineering – the averaging of fast periodic modulations to obtain an effective time-independent system – is an ubiquitous tool for the manipulation and probing of various systems, ranging from NMR probes in solid state physics to atom-light interactions or Raman-dressed states [1]. In recent years, Floquet techniques have established themselves as a toolbox for the creation of novel Hamiltonians for ultra-cold atoms in optical lattices, including lattice shaking [2–8], Raman-assisted hopping [9–12], and modulated interactions [13–18].

A major reason for the interest on Floquet techniques lies in the possibility of engineering gauge fields, i.e. complex hopping rates, for neutral atoms in optical lattices [7]. Most relevantly, synthetic magnetic fields have been created in the last years using Raman-assisted hopping [9–12]. Interestingly, various Floquet techniques have been recently proposed for the creation of occupation-dependent gauge fields (ODG) [19–22], in which the phase of the hopping depends on the site occupation. Under proper conditions, 1D models with ODG may be mapped into an anyon-Hubbard model (AHM) [19–22], in which the exchange statistics of the atoms may be externally modified. The 1D AHM presents a wealth of new physics, including statistically-induced transitions [20], novel superfluid phases [21], smooth fermionization [22], asymmetric momentum distributions [23, 24], and intriguing dynamics [25–27]. The atomic back-action on the synthetic gauge field given by ODG could pave a way for the realization of dynamical gauge fields [28, 29], and leads to interesting physics, such as chiral solitons in Bose-Einstein condensates [30] or density-flux interplay in 2D lattices [31].

In this Letter we propose a novel method based on the multi-color modulation of the depth of a tilted optical lattice. As shown by Ma et al. [32] lattice-depth modulations may be employed to assist different occupation-dependent hoppings for sufficiently strong interactions. We show for the particular case of two-component fermions that a three-color modulation (3CM) of the lattice depth may be employed to achieve a separate flexible control of correlated hopping, ODG, effective on-site interactions without the need of Feshbach resonances, and nearest-neighbor interactions. As a result, 3CM allows with a minimal experimental complexity for engineering a broad class of lattice Hamiltonians using ultra cold atoms, including Hubbard models with correlated hopping, peculiar extended models, and two-component AHM, whose basic properties we analyze as well.

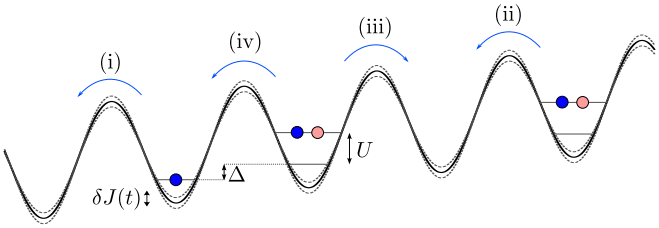

FIG. 1: (Color online) Sketch of the lattice set-up and the relevant hoppings.

Effective Hamiltonian.– We consider a balanced two-component ($\sigma = \uparrow, \downarrow$) Fermi gas in an optical lattice (equal for both components), whose depth is modulated in time, $V(t) = V_0 + \delta V(t)$, with $\delta V \ll V_0$. We choose two-component fermions for simplicity, but similar ideas may be applied to bosons, and multi-component fermions. In the tight-binding regime, the hopping rate is $\frac{J(s)}{E_{rec}} = \frac{4}{\sqrt{\pi}} s^{3/4} \exp(-2\sqrt{s})$ [33], where $s = V/E_{rec} = s_0 + \delta s(t)$, with E_{rec} the recoil energy associated to the laser that creates the lattice. Since $\delta s \ll s_0$, then $J(t) = J_0 + \delta J(t)$, where $J_0 = J(s_0)$, and $\frac{\delta J(t)}{J_0} = \left(\frac{3}{4} - \sqrt{s_0}\right) \frac{\delta s(t)}{s_0}$, and hence the lattice modulation directly maps into a modulation of the hopping rate. We assume a tilted lattice, with an energy shift Δ between neighboring sites (Fig. 1). The system is then described by the Fermi-Hubbard Hamiltonian:

$$\mathcal{H}(t) = -J(t) \sum_{j,\sigma} \left[c^\dagger_{j+1,\sigma} c_{j,\sigma} + \text{H.c.} \right] + U \mathcal{H}_{\text{int}} + \Delta \mathcal{H}_{\text{tilt}}, \quad (1)$$

where $c_{j,\sigma}$ is the annihilation operator of a fermion with spin σ at site j, U characterizes the on-site interactions, $\mathcal{H}_{\text{int}} = \sum_j n_{j,\uparrow} n_{j,\downarrow}$, and $\mathcal{H}_{\text{tilt}} = \sum_{j,\sigma} j n_{j,\sigma}$. Note that four different hoppings are possible (Fig. 1): (i) a single atom hops to an empty site to its right leading to an energy

shift $\Delta E_1 = \Delta$; (ii) an atom with spin σ, initially alone at a given site, tunnels to the site at its right already occupied by a single atom with $\bar{\sigma} \neq \sigma$, resulting in a shift $\Delta E_2 = \Delta + U$; (iii) same as (ii) but the hopping is to the left – in this case $\Delta E_3 = U - \Delta$; and (iv) an atom of component σ sharing a site with a $\bar{\sigma}$ atom, tunnels into the site at its right already occupied by a single atom with $\bar{\sigma}$ leading to $\Delta E_4 = \Delta$ (i.e. (iv) and (i) are resonant).

We assume that $J(t) \ll \Delta, |\Delta \pm U|$, and hence direct hopping is negligible. However, a periodic modulation of $\delta J(t)$ leads to assisted hopping if the modulation frequency matches the energy shift associated to the hopping process [32]. Crucially, processes (i), (ii) and (iii) are characterized by different energy shifts (typically separated by several kHz, see below), and hence the different hoppings may be laser-assisted separately. The key point of our proposal is to address them separately but simultaneously using a 3CM of the laser intensity: $\delta V(t) = \sum_{s=1,2,3} \delta V_s \cos(\omega_s t + \phi_s)$, which, as mentioned above, translates into an equivalent modulation of the hopping, $\delta J(t) = \sum_s \delta J_s \cos(\omega_s t + \phi_s)$. Each component of the modulation has an amplitude δJ_s and a dephase $\delta\phi_s$, which may be independently controlled. The frequencies $\omega_1 = \Delta$, $\omega_2 = \Delta + U - \tilde{U}$, and $\omega_3 = -\Delta + U - \tilde{U}$, with $|\tilde{U}| \ll U$ are chosen (quasi-)resonant to the hoppings (i) (and hence also (iv)), (ii), and (iii), respectively.

In interaction picture, $\tilde{\mathcal{H}} = \mathcal{U}^\dagger \mathcal{H} \mathcal{U}$, with $\mathcal{U} = \exp\left[-it(\Delta \mathcal{H}_{\rm tilt} + U \mathcal{H}_{\rm int})\right]$:

$$\tilde{\mathcal{H}}(t) = J(t) \sum_{j,\sigma} \left[c^\dagger_{j,\sigma} e^{it[\Delta + U(n_{j,\bar{\sigma}} - n_{j+1,\bar{\sigma}})]} c_{j+1,\sigma} + \text{H.c.} \right]. \quad (2)$$

3CM introduces oscillating terms $e^{\pm i(\omega_s \pm \Delta E_{s'})t}$. For $|\Delta - U|, U \gg J_0$ the fast-oscillating terms average to zero (rotating wave approximation (RWA)), and only quasi-resonant terms remain [34]. As a result, processes (i) (and (iv)), (ii), and (iii) present an effective hopping rate $\frac{\delta J_s}{2} e^{i\phi_s}$, with $s = 1$, 2, and 3, respectively. We consider below the particular case with $\delta J_{2,3} = \beta\, \delta J_1$, $\phi_1 = 0$, $\phi_{2,3} = \phi$. Undoing the interaction picture we obtain the effective time-independent Hamiltonian:

$$\mathcal{H}_{eff} = -\frac{\delta J_1}{2} \sum_{\sigma,j} c^\dagger_{j+1,\sigma} F[|n_{\bar{\sigma},j+1} - n_{\bar{\sigma},j}|] c_{j,\sigma} + \tilde{U} \mathcal{H}_{int}, \quad (3)$$

where $F[0] = 1$, and $F[1] = \beta e^{i\phi}$. 3CM provides remarkable control possibilities. Both the amplitude and the phase of the hopping rate of the σ component depend on the site occupation of the $\bar{\sigma}$ component. As shown below, this may be employed to realize ODG. Moreover, the detuning $\tilde{U}$ results in an effective on-site interaction, allowing for controlling interactions even in those systems where Feshbach resonances are not available. This is in particular the case of alkaline-earth fermions in the lowest $^1S_0$ state [35]. Since 3CM may be also used with multi-component fermions, this opens a novel way of controlling the properties of SU(N) fermions [35].

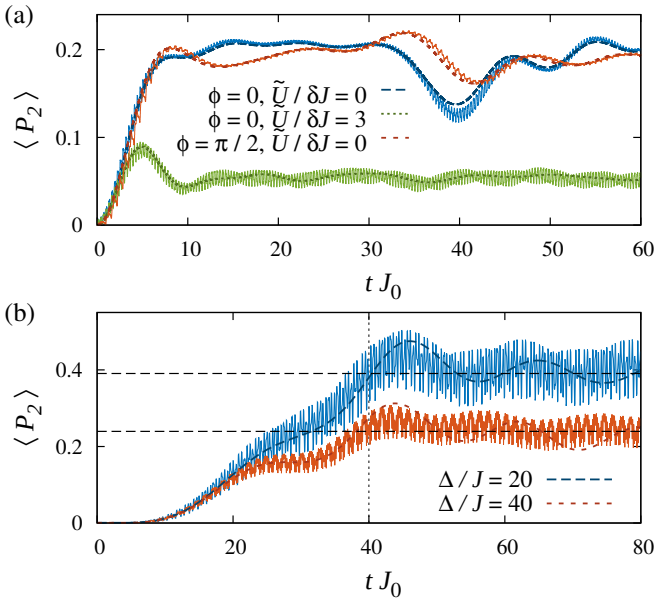

FIG. 2: (Color online) (a) Average double occupancy $\langle P_2 \rangle$ after a sudden-quench of δV for a finite temperature $T = J_0$, $\Delta/J_0 = 20$, $U/J_0 = 10$, $\delta J_1/J_0 = 0.2$, $\beta = 1$, and different values of $\tilde{U}/\delta J_1$ and ϕ (exact diagonalization results using 6 particles in 6 sites); dashed (solid) curves depict the results of the effective (full) model; (b) $\langle P_2 \rangle$ for a quasi-adiabatic preparation (iTEBD results for $\rho = 1$). The system is initially prepared in a MI for $\delta V = 0$. $\delta V(t)$ is linearly increased to its final value for $0 < J_0 t < 40$; we consider $U/J_0 = 5$, $\delta J_1/J_0 = 0.1, \tilde{U}/\delta J_1 = 2$, $\beta = 1$. $\langle P_2 \rangle(t)$ for the full (solid) and effective model (dashed) oscillates around the expected value (horizontal lines) for the ground state with the final δV.

Although for $J(t) \ll \Delta, |\Delta \pm U|$ direct hoppings are energetically forbidden, virtual hoppings may induce effective interactions between NN sites [34] of the form

$$\begin{aligned} \mathcal{H}_{NN} = \sum_{\langle i,j \rangle} \Bigg[& \frac{2J_0^2}{\Delta + U} P_i^0 P_j^2 - \frac{2J_0^2}{\Delta - U} P_i^2 P_j^0 \\ & + \frac{J_0^2}{\Delta} \left((1 - n_i) P_j^1 - P_i^1 (1 - n_j) \right) \\ & + \frac{2U J_0^2}{\Delta^2 - U^2} (P_i^{1\uparrow} P_j^{1\downarrow} + P_i^{1\downarrow} P_j^{1\uparrow} - S_i^+ S_j^- - S_i^- S_j^+) \Bigg], \end{aligned} \quad (4)$$

where $S_i^+ = c^\dagger_{i,\uparrow} c_{i,\downarrow}$ and $S_i^- = c^\dagger_{i,\downarrow} c_{i,\uparrow}$ are spin operators, $n_i = n_{i,\downarrow} + n_{i,\uparrow}$, and we introduce the projector of two particles per site $P_i^2 = n_{i,\downarrow} n_{i,\uparrow}$, zero particles $P_i^0 = (1 - n_{i,\downarrow})(1 - n_{i,\uparrow})$, and a single particle $P_i^{1\sigma} = (1 - n_{i,\bar{\sigma}}) n_{i,\sigma}$, and $P_i^1 = P_i^{1\downarrow} + P_i^{1\uparrow}$. The peculiar NN interactions depend on J_0^2/Δ and $J_0^2/(U \pm \Delta)$, whereas the effective hopping is given by δJ_i. Hence they may be separately controlled. For sufficiently small $J_0 \ll \Delta, |U \pm \Delta|$ we may neglect $\mathcal{H}_{NN}$. However, as shown below, $\mathcal{H}_{NN}$ opens additional interesting possibilities.

Non-equilibrium dynamics.– Figure 2(a) depicts our results for the dynamics of the averaged probability of

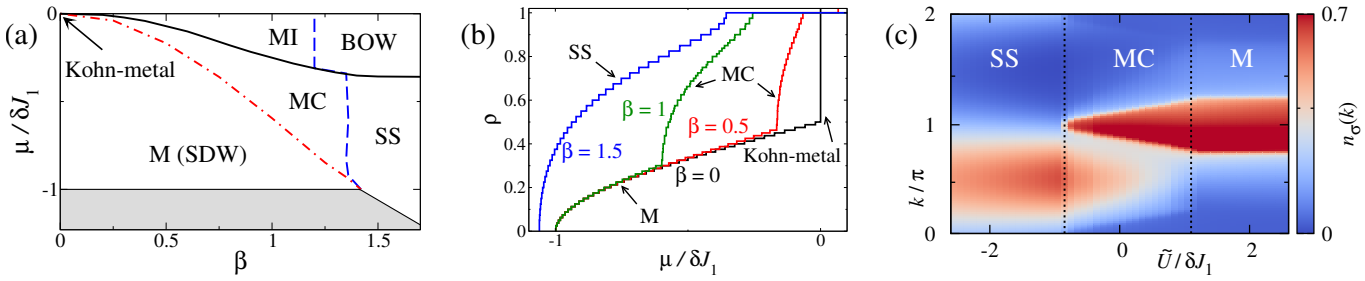

FIG. 3: (Color online) (a) Phase diagram of $\mathcal{H}_{eff}$ as function of $\mu/\delta J_1$ and β for $\phi = \pi/2$ and $\tilde{U} = 0$ [46]. The dash-dotted lines mark the C-IC M-MC transition. The dashed (blue) lines denote the opening of Δ_S that marks the MC-SS and MI-BOW transitions. Shaded regions depict the vacuum. (b) Equation of state $\rho = \rho(\mu)$ for $\beta = 0$, 0.5, 1, and 1.5 for the parameters of Fig. (a). (c) Momentum distribution $n_\sigma(k)$ of Eq. (5) for $\rho = 0.5$, and $\phi = \pi/2$ ($L = 60$).

double occupancy, $\langle P_2\rangle$, based on exact diagonalization of small systems [36]. We initially prepare for $\delta V = 0$ a Mott-insulator (MI) state at $U \gg J_0$, assuming an initial temperature $T = J_0$, and hence initially $\langle P_2\rangle \simeq 0$. At time $t = 0$ we abruptly turn on the modulation $\delta J(t)$. The results show a very good agreement between the effective model $\mathcal{H}_{eff} + \mathcal{H}_{NN}$, and the full model (1). Figure 2(a) shows that non-equilibrium experiments should be able to reveal both the ODG, and the suppression of $\langle P_2\rangle$ resulting from the repulsive effective interactions $\tilde{U}$.

The analysis of ground-state properties requires a (quasi-)adiabatic ramping of δV. We present in Fig. 2(b) our results obtained using infinite time evolving block decimation (iTEBD) [37]. Starting again with $\delta V = 0$ from an initial MI state, we have studied the quasi-adiabatic preparation of different MI states. During the time $0 < t < t_{\rm ramp}$ we linearly increase δV to its final value, monitoring $\langle P_2\rangle$. Again $\mathcal{H}_{eff} + \mathcal{H}_{NN}$ reproduces very well the dynamics of the full model (1). After the ramp, the heating induced by the quasi-adiabatic character of the finite ramping time results in oscillations of $\langle P_2\rangle$ around the value expected for the ground state of the effective model (see below).

Phases of the effective Hamiltonian.– At this point we focus on the ground-state physics of $\mathcal{H}_{eff}$, assuming that $J_0 \ll \Delta, |\Delta \pm U|$, and hence that $\mathcal{H}_{NN}$ may be neglected. For $\beta \neq 1$, $\mathcal{H}_{eff}$ realizes a broad class of Hubbard models with correlated hopping extensively studied in the context of cuprate superconductors [38–42], and recently revisited for ultra-cold gases with modulated interactions [16, 17]. For $\phi \neq 0$, the ODG gives rise to a particularly intriguing physics. For $\beta = 1$:

$$\mathcal{H}_{eff} = -\frac{\delta J_1}{2}\sum_{\sigma,j} c^\dagger_{j+1,\sigma} e^{i\phi|n_{\bar\sigma,j+1}-n_{\bar\sigma,j}|} c_{j,\sigma} + \tilde{U}\mathcal{H}_{int}. \quad (5)$$

For a low lattice filling ρ for which processes (iv) may be neglected, a Jordan-Wigner like transformation [20], $f_j = e^{i2\phi\sum_{1\le l<j} n_l} e^{i\phi n_j} c_j$, maps (5) into a two-component anyon-Hubbard model (2-AHM):

$$\mathcal{H}_{AHM} = -\frac{\delta J_1}{2}\sum_{j,\sigma}(f^\dagger_{j,\sigma} f_{j+1,\sigma} + \text{H.c.}) + \tilde{U}\mathcal{H}_{int}\,. \quad (6)$$

where the operators $f_{j,\sigma}$ and $f^\dagger_{j,\sigma}$ characterize anyon-like hardcore particles that fulfill a deformed exchange statistics (DES): $f_{j,\sigma} f_{k,\sigma'} + \mathcal{Q}^{\sigma,\sigma'}_{j,k} f^\dagger_{k,\sigma'} f_{j,\sigma} = \delta_{jk}\delta_{\sigma,\sigma'}$ and $f_{j,\sigma} f_{k,\sigma'} + \mathcal{Q}^{\sigma,\sigma'}_{j,k} f_{k,\sigma'} f_{j,\sigma} = 0$, with $\mathcal{Q}^{\sigma,\sigma'}_{j,k} = e^{i2\phi}$ ($j > k$), 0 ($j = k$), $e^{-i2\phi}$ ($j < k$). Specific cases of the 2-AHM have been studied in the context of exactly solvable models [43, 44]. In contrast, the non-integrable DES discussed here does strongly modify the spectrum of the 2-AHM compared to the fermionic Hubbard model.

Figure 3(a) shows, as a function of β and the chemical potential μ, the ground-state phase diagram of (5) for $\phi = \pi/2$ and $\tilde{U} = 0$, obtained by means of density matrix renormalization group (DMRG) [45] simulations in finite-size open-boundary systems of up to 80 sites, keeping up to 600 matrix states [46]. For $\beta = 0$ doubly-occupied sites (doublons) and empty ones (holons) become mutually impenetrable, resulting at half filling in a non-conducting metal with a vanishing Drude weight (Kohn metal) [39]. For $0 < \beta < 1$, in the absence of ODG, the system undergoes a smooth phase transition from a metal (M) with dominant spin-density wave (SDW) correlations, $(-1)^j\langle n_{0-} n_{j-}\rangle$, with $n_{j-} = n_{j,\uparrow} - n_{j,\downarrow}$, to a triplet superconductor [17]. On the contrary, for $\phi = \pi/2$, the M phase undergoes for $\beta \lesssim 1.4$ a commensurate-incommensurate (C-IC) phase transition, marked by a kink in the $\mu(\rho)$ curve (Fig. 3(b)), to a peculiar gapless multi-component (MC) phase. The MC phase presents a central charge $c \approx 3$ [47–49]. In contrast, the metallic phase has $c = 2$. The MC phase smoothly connects to the Kohn-metal for $\beta \to 0$. For $\beta \gtrsim 1.4$ and $\rho \neq 1$, a spin gap Δ_S opens and the kink in $\mu(\rho)$ disappears marking the transition to a phase with dominant singlet-superconducting (SS) correlations, $\langle \mathcal{Q}^\dagger_{0-}\mathcal{Q}_{j-}\rangle$, with $\mathcal{Q}_{j-} \equiv c_{j+1,\downarrow}c_{j,\uparrow} - c_{j+1,\uparrow}c_{j,\downarrow}$. Finally, at $\rho = 1$ we find a MI with dominant SDW correlations, and a totally gapped phase with bond-ordering

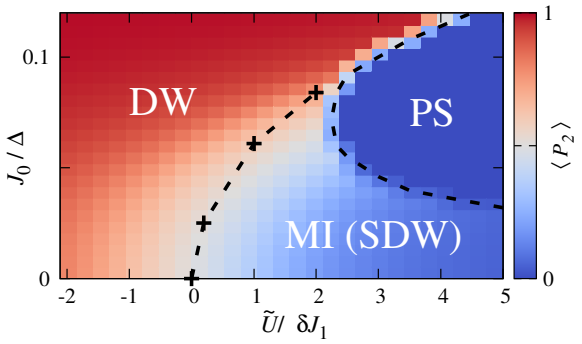

FIG. 4: (Color online) Phase diagram of $\mathcal{H}_{eff} + \mathcal{H}_{NN}$ for $\rho = 1$, $U = 5J_0$, $\delta J = 0.1J_0$, $\beta = 1$, and $\phi = 0$. The MI-DW transition is given by $K_S = 1$ (extrapolated from DMRG calculations of up to $L = 160$ sites [51]). The coloring codes $\langle P_2 \rangle$ obtained from iTEBD calculations (for 200 states results are consistent with our DMRG data of 160 sites).

wave (BOW) order $\mathcal{O}_D(x) = \sum_\alpha T_\alpha(x) - T_\alpha(x+1)$, with $T_\alpha(x) = c^\dagger_{\alpha,x} c_{\alpha,x+1} + H.c.$.

MC phase.– The MC phase, which occurs even for $\beta = 1$ and $\tilde{U} = 0$, is a direct consequence of the ODG. The nature of this phase is best understood for $\phi = \pi/2$ and $\beta = 1$. In that case, the two-particle problem, with a $\uparrow$ particle and a $\downarrow$ one, presents for any $\tilde{U}$ an exact bound eigenstate, $|P\rangle = \cos\theta|D\rangle + \mathrm{i}\sin\theta|S\rangle$, with energy $E_P = \frac{\tilde{U}}{2} - \sqrt{\frac{\tilde{U}^2}{4} + 2\delta {J_1}^2}$, where $\tan\theta = \frac{\tilde{U} - E_P}{\sqrt{2}\delta J_1}$, $|D\rangle = \sum_j (-1)^j |\uparrow,\downarrow\rangle_j$, and $|S\rangle = \sum_j (-1)^j (|\uparrow\rangle_j |\downarrow\rangle_{j+1} - |\downarrow\rangle_j |\uparrow\rangle_{j+1})/\sqrt{2}$. The existence of this bound state even for $\tilde{U} > 0$ results from the ODG (see Suppl. Material [34]). For sufficiently large $\tilde{U} > 0$, $E_P > 2E_F$, with E_F the Fermi energy of the metal, and the M phase is stable. For decreasing $\tilde{U}$, $E_P < 2E_F$, and part of the Fermi sea forms pairs that quasi-condense in $|P\rangle$, until the new Fermi energy $E'_F = E_P/2$. The MC phase results from the coexistence of a partially depleted Fermi sea and bound pairs. When E'_F reaches the bottom of the lattice band, the Fermi sea is fully depleted marking the onset of the SS phase.

The MC phase has a characteristic momentum distribution of both components, $n_\sigma(k)$, and it can be thus easily revealed in time-of-flight measurements. Figure 3(c) shows our results for $n_\sigma(k)$ for $\phi = \pi/2$. For large-enough $\tilde{U}$ the M phase presents a slab-like Fermi sea. In the MC phase, the slab shrinks due to partial pairing. The latter results in a blurred contribution to $n_\sigma(k)$, $\frac{1}{2\pi}\left[1 - \sqrt{2}\sin(2\theta)\sin(k/2) - \sin^2\theta\cos(2k)\right]$, as expected for $|P\rangle$ pairs [34]. The MC-SS transition is marked by the vanishing Fermi sea.

Intersite interactions.– $\mathcal{H}_{NN}$ becomes relevant for large-enough J_0/Δ, $J_0/|\Delta \pm U|$. Combining effective on-site and NN interactions constitutes an additional interesting control possibility resulting from the 3CM. Figure 4 depicts for $\beta = 1$, $\phi = 0$ and $\rho = 1$ the phase diagram as a function of $\tilde{U}/\delta J$, and J_0/Δ (which controls the strength of the NN terms). For $J_0/\Delta \to 0$ the standard two-component 1D Fermi Hubbard model is recovered [50]. For any $\tilde{U} > 0$ there is a MI (SDW) phase with a finite charge excitation gap $\Delta_c > 0$ but $\Delta_S = 0$, whereas for $\tilde{U} < 0$ $\Delta_S > 0$ and $\Delta_c = 0$. For sufficiently large J_0/Δ the system is driven into a fully gapped density-wave (DW), characterized by a non-vanishing DW order $(-1)^j \langle n_0 n_j \rangle$. For $\tilde{U} > 0$ we observe two MI phases with a suppressed doublon number, the above mentioned MI (SDW) and a region of phase separation of ferromagnetic domains (PS). The MI-DW transition is associated to the opening of Δ_S, characterized by the Luttinger-liquid parameter in the spin sector $K_S = 1$ (+-symbols in Fig. 4) [51, 52]. Since $\mathcal{H}_{NN}$ breaks the spatial reflection symmetry, we do not observe a separate BOW phase, as it is the case for Hubbard models with standard density-density NN interactions [53], but a non-zero BOW-order in the DW due to the preferred creation of excitations in a particular spatial direction.

Outlook.– A multicolor modulation of the lattice depth allows for a flexible separate manipulation of (a) correlated hopping, controlled by the modulation amplitudes δV_s; (b) ODG, given by the dephasings ϕ_s; (c) effective on-site interactions, provided by the detuning $\tilde{U}$; and (d) NN interactions, that depend on J_0/Δ and $J_0/|\Delta \pm U|$. 3CM thus provides an experimentally straightforward method for engineering a very broad class of lattice models, including Hubbard Hamiltonians with correlated hopping, peculiar extended models, and 2-AHM. In particular, the controllable quantum statistics of the 2-AHM results in a peculiar MC phase of coexisting superconducting and metallic components. The RWA requirements necessary for the 3CM are readily achievable experimentally. For example, for ^{173}Yb (scattering length of $199.4a_B$ and lattice spacing of 380nm [11, 54]) with $s_0 = 6.9$ ($J_0/h = 100$Hz), one achieves $U = 23J_0$, $\Delta = 16J_0$, $|\Delta - U| = 7J_0$, well within the RWA requirements. For $\delta J/J_0 = 0.2$, the typical effective-tunneling time is $\tau = \hbar/\delta J \simeq 8$ ms.

Multi-color modulation permits several further interesting extensions, including the control of three-body interactions [55]. In combination with a Raman-induced coupling of several spin components [11, 12] one may study density dependent magnetic fields [31]. Other scenarios could pave a realistic exploration path towards the simulation of dynamical gauge fields with cold atoms in optical lattices, exploring e.g. occupation-dependent non-Abelian fields and gauge fields in Fermi-Bose mixtures.

We thank L. Fallani, A. Eckardt, and C. de Morais-Smith for discussions. We acknowledge support of QUEST-LFS and the DFG Research Training Group 1729. Simulations were carried out on the cluster system at the Leibniz University of Hannover, Germany.

[1] P. Hänggi, in *Quantum Transport and Dissipation*, edited by T. Dittrich et al. (Wiley-VCH, New York, 1998), Chap. 5.
[2] A. Eckardt, C. Weiss, and M. Holthaus. Phys. Rev. Lett. **95**, 260404 (2005).
[3] H. Lignier *et al.* Phys. Rev. Lett. **99**, 220403 (2007).
[4] E. Kierig *et al.*, Phys. Rev. Lett. **100**, 190405 (2008).
[5] A. Zenesini *et al.* Phys. Rev. Lett. **102**, 100403 (2009).
[6] J. Struck *et al.*, Science **333**, 996 (2011).
[7] J. Struck *et al.*, Phys. Rev. Lett. **108**, 225304 (2012).
[8] C. V. Parker, L .C. Ha, and C. Chin, Nature Physics **9**, 769 (2013).
[9] M. Aidelsburger *et al.*, Phys. Rev. Lett. **111**, 185301 (2013).
[10] H. Miyake *et al.*, Phys. Rev. Lett. **111**, 185302 (2013).
[11] M. Mancini *et al.*, Science **349**, 1510 (2015).
[12] B.K. Stuhl *et al.*, Science **349**, 1514 (2015).
[13] J. Gong, L. Morales-Molina, and P. Hänggi, Phys. Rev. Lett. **103**, 133002 (2009).
[14] F. K. Abdullaev, P. G. Kevrekidis, and M. Salerno, Phys. Rev. Lett. **105**, 113901 (2010).
[15] Á. Rapp, X. Deng, and L. Santos, Phys. Rev. Lett. **109**, 203005 (2012).
[16] M. Di Liberto, C. E. Creffield, G. I. Japaridze, and C. Morais-Smith, Phys. Rev. A **89**, 013624 (2014).
[17] S. Greschner, L. Santos, and D. Poletti, Phys. Rev. Lett. **113**, 183002 (2014).
[18] F. Meinert *et al.*, arXiv:1602.02657 (2016).
[19] S. Greschner, G. Sun, D. Poletti, and L. Santos, Phys. Rev. Lett. **113**, 215303 (2014).
[20] T. Keilmann, S. Lanzmich, I. McCulloch, and M. Roncaglia, Nature Commun. **2**, 361 (2011).
[21] S. Greschner and L. Santos, Phys. Rev. Lett. **115**, 053002 (2015)
[22] C. Sträter, S. C. Srivastava, and A. Eckardt, arXiv:1602.08384 (2016).
[23] Y. Hao, Y. Zhang, and S. Chen, Phys. Rev. A **79**, 043633 (2009).
[24] G. Tang, S. Eggert, and A. Pelster, New J. of Phys. **17**, 123016 (2015).
[25] A. del Campo, Phys. Rev. A **78**, 045602 (2008).
[26] Y. Hao, and S. Chen, Phys. Rev. A **86**, 043631 (2012).
[27] L. Wang, L. Wang, and Y. Zhang, Phys. Rev. A **90**, 063618 (2014).
[28] U. J. Wiese, Ann. der Physik **525**, 777 (2013).
[29] A. Bermudez, and D. Porras, New J. of Phys. **17**, 103021 (2015).
[30] M. Edmonds *et al.*, Phys. Rev. Lett. **110**, 085301 (2013).
[31] S. Greschner *et al.*, Phys. Rev. B **92**, 115120 (2015).
[32] R. Ma *et al.*, Phys. Rev. Lett. **107**, 095301 (2011).
[33] W. Zwerger, J. Opt. B: Quantum Semiclass. Opt. **5**, 9 (2003).
[34] See the Suppl. Material for further details about the MC phase and an alternative derivation of the effective time-independent model using Magnus expansion.
[35] See M. A. Cazalilla and A. M. Rey, Rep. Prog. Phys. **77**, 124401 (2014), and references therein.
[36] Similar agreement between the dynamics of the full model and the effective one is obtained in the thermodynamic limit employing infinite time evolving block decimation (iTEBD) simulations [37], which are possible using the translational invariant formulation of Eq. (2).
[37] G. Vidal, Phys. Rev. Lett. **98**, 070201 (2007).
[38] L. Arrachea and A. A. Aligia, Phys. Rev. Lett. **73**, 2240 (1994).
[39] L. Arrachea, A. A. Aligia, and E. Gagliano, Phys. Rev. Lett. **76**, 4396 (1996).
[40] L. Arrachea, E. R. Gagliano, and A. A. Aligia, Phys. Rev. B **55**, 1173 (1997).
[41] A. A. Aligia and L. Arrachea, Phys. Rev. B **60**, 15332 (1999).
[42] A. A. Aligia, K. Hallberg, C. D. Batista, and G. Ortiz, Phys. Rev. B **61**, 7883 (2000).
[43] H. J. Schulz and G. S. Shastry, Phys. Rev. Lett. **80**, 1924 (1998).
[44] A. Osterloh, L. Amico, and U. Eckern, J. of Phys. A: Mathematical and General **33**, L87 (2000).
[45] U. Schollwöck, Ann. of Physics **326**, 96 (2011).
[46] Hamiltonian (3) is symmetric under particle-hole exchange, and hence the region $\mu > 0$ ($\rho > 1$) is mirror symmetric to that depicted for $\mu < 0$ ($\rho < 1$) in Fig. 3(a).
[47] We evaluate the central charge from the conformal expression of the von-Neumann entropy, $S_{vN,L}(l) = \frac{c}{3} \ln \left[\frac{L}{\pi} \sin \left(\frac{\pi}{L} l \right) \right] + \gamma$, for a subsystem of length l in a system of L sites, with γ a constant [48, 49].
[48] G. Vidal, J. I. Latorre, E. Rico, and A. Kitaev, Phys. Rev. Lett. **90**, 227902 (2003).
[49] P. Calabrese and J. Cardy, J. Stat. Mech. P06002 (2004).
[50] F. H. Essler, H. Frahm, F. Göhmann, A. Klümper, and V. E. Korepin, *The one-dimensional Hubbard model*, Cambridge University Press (2005).
[51] We extract K_s from the long wavelength behavior of the static spin structure factor, $\frac{1}{L} \sum_{i,j} e^{\mathrm{i}(i-j)k} \langle n_{i-} n_{j-} \rangle$ [52].
[52] A. Moreno, A. Muramatsu, and S. R. Manmana, Phys. Rev. B **83**, 205113 (2011).
[53] S. Ejima and S. Nishimoto, Phys. Rev. Lett. **99**, 216403 (2007).
[54] M. Höfer *et al.*, Phys. Rev. Lett. **115**, 265302 (2015).
[55] A. Daley and J. Simon, Phys. Rev. A **89**, 053619 (2014).

arXiv:1604.08829v1 [cond-mat.quant-gas] 29 Apr 2016

Supplementary material for "Engineering interactions and anyon statistics by multicolor lattice-depth modulations"

Lorenzo Cardarelli,[1] Sebastian Greschner,[1] and Luis Santos[1]

[1]*Institut für Theoretische Physik, Leibniz Universität Hannover, Appelstr. 2, DE-30167 Hannover, Germany*

In this Supplementary Material we discuss in more detail about the physics of the multi-component (MC) phase. We comment as well in more detail about the derivation of the effective Hamiltonian using a Magnus expansion.

I. MULTI-COMPONENT PHASE

A. Two-particle model

We assume for simplicity $\beta = 1$, and hence Model (5) of the main text. We are interested in the two-particle problem, with one $\uparrow$ particle and one $\downarrow$ particle. Let $|D(j)\rangle$ be a doubly ocuppied site (j site), and $|S(j,j+l)\rangle$ a singlet state placed in sites j and $j+l$. Then

$$\mathcal{H}_{eff}|D(j)\rangle = -\frac{\delta J_1}{\sqrt{2}}\left[e^{\mathrm{i}\phi}|S(j,j+1)\rangle + e^{-\mathrm{i}\phi}|S(j-1,j)\rangle\right] + \tilde{U}|D(j)\rangle, \tag{1}$$

$$\mathcal{H}_{eff}|S(j,j+1)\rangle = -\frac{\delta J_1}{\sqrt{2}}\left[e^{\mathrm{i}\phi}|D(j+1)\rangle + e^{-\mathrm{i}\phi}|D(j)\rangle\right] - \frac{\delta J_1}{2}\left[|S(j-1,j+1)\rangle + |S(j,j+2)\rangle\right], \tag{2}$$

$$\mathcal{H}_{eff}|S(j,j+l)\rangle \overset{l\geq 1}{=} -\frac{\delta J_1}{2}\left[|S(j-1,j+l)\rangle + |S(j+1,j+l)\rangle + |S(j,j+l-1)\rangle + |S(j,j+l+1)\rangle\right]. \tag{3}$$

Let $|D(k)\rangle = \frac{1}{\sqrt{L}}\sum_l e^{\mathrm{i}kl}|D(l)\rangle$ and $|S(j,k)\rangle = \frac{1}{\sqrt{L}}\sum_l e^{\mathrm{i}k(l+j/2)}|S(l,l+j)\rangle$, with k the center-of-mass momentum of the pair, and L the number of sites. Then $\mathcal{H}_{eff} = \sum_k \mathcal{H}_{eff}(k)$, with $\mathcal{H}_{eff}(k) = \mathcal{H}_0(k) + \mathcal{H}_1(k)$, where:

$$\mathcal{H}_0(k) = \tilde{U}|D(k)\rangle\langle D(k)| - A(k)\left[|S(1,k)\rangle\langle D(k)| + h.c.\right], \tag{4}$$

$$\mathcal{H}_1(k) = -B(k)\sum_{j\geq 1}\left[|S(j,k)\rangle\langle S(j+1,k)| + h.c.\right], \tag{5}$$

with $A(k) = \sqrt{2}\delta J_1\cos(k/2-\phi)$ and $B(k) = \delta J_1\cos(k/2)$. We may diagonalize $\mathcal{H}_0$:

$$\mathcal{H}_0(k) = E_+(k)|\tilde{P}(k)\rangle\langle\tilde{P}(k)| + E_-(k)|P(k)\rangle\langle P(k)|, \tag{6}$$

where the eigenenergies are $E_\pm(k) = \frac{\tilde{U}}{2} \pm \sqrt{\left(\frac{\tilde{U}}{2}\right)^2 + A(k)^2}$, and the corresponding eigenstates are $|\tilde{P}(k)\rangle = \cos\theta(k)|D(k)\rangle + \sin\theta(k)|S(1,k)\rangle$, and $|P(k)\rangle = -\sin\theta(k)|D(k)\rangle + \cos\theta(k)|S(1,k)\rangle$, with $\tan\theta(k) = \frac{\tilde{U}/2 - E_-(k)}{A(k)}$. The Hamiltonian $\mathcal{H}_0$ characterizes deeply-bound pairs. We may then split $\mathcal{H}_1(k) = \mathcal{H}_c(k) + \mathcal{H}_u(k)$, where

$$\mathcal{H}_u(k) = -B(k)\sum_{j\geq 2}\left[|S(j,k)\rangle\langle S(j+1,k)| + h.c.\right] \tag{7}$$

determines the physics of broken pairs, where the dynamics of relative coordinate j is given by the hopping rate $B(k)$, and

$$\mathcal{H}_c(k) = -B(k)\left(\sin\theta(k)|P(k)\rangle + \cos\theta(k)|\tilde{P}(k)\rangle\right)\langle S(2,k)| + h.c, \tag{8}$$

characterizes the coupling between deeply-bound and unbound pairs. Note that such a coupling is also given by $B(k)$.

Let us consider $\phi = \frac{\pi}{2}$. In that case, $E_\pm(k) = \frac{\tilde{U}}{2} \pm \sqrt{\left(\frac{\tilde{U}}{2}\right)^2 + 2\delta J_1^2\sin^2(k/2)}$. The minimal energy is clearly for $k = \pi$, $E_P \equiv E_-(\pi) = \frac{\tilde{U}}{2} \pm \sqrt{\left(\frac{\tilde{U}}{2}\right)^2 + 2\delta J_1^2}$. If existing, bound pairs will quasi-condense in $|P\rangle \equiv |P(\pi)\rangle$. Crucially, $B(\pi) = 0$, and hence $\mathcal{H}_c = 0$. As a result, $|P\rangle$ remains a deeply-bound two-particle eigenstate, fully decoupled from the unbound pairs, irrespective of the value of $\tilde{U}/\delta J_1$. On the contrary for $\phi = 0$, i.e. without occupation-dependent gauge (ODG), the bound pairs

are fully connected with the rest and cannot be formed unless $\tilde{U} < 0$ dominates. For ϕ in the vicinity of $\pi/2$ the coupling $\mathcal{H}_c$ may be considered perturbative, and deeply-bound pairs due to the ODG still exist even if ϕ is not exactly $\pi/2$.

The existence of these pairs that are deeply-bound by the ODG rather than by attractive interactions is crucial to understand the nature of the MC phase. The metallic (M) phase is stable if $E_P/2 > E_F$, with E_F the Fermi energy of the metal. However, for decreasing $\tilde{U} > 0$, $E_F < E_P/2$, and hence it is energetically favorable to pair part of the Fermi sea into $|P\rangle$ pairs, until reaching an equilibrium at a new Fermi energy $E'_F = E_P/2$. This partial pairing, and the corresponding coexistence of a two-component metal and a superconductor explains the MC phase, and its $c = 3$ central charge. For $E_-(\pi) < -2\delta J_1$ (which occurs at $\tilde{U}/\delta J_1 \simeq -1$) the Fermi sea is completely depleted, and the system enters the fully-paired (SS) phase.

B. Momentum distribution

The momentum distribution of the $\uparrow$ component in the $|P\rangle$ state is $n_\uparrow^{(P)}(k) = \sum_{i,j} e^{\mathrm{i}k(i-j)} \langle P|c_{i,\uparrow}^\dagger c_{j,\uparrow}|P\rangle$, where

$$\langle P|c_{l,\uparrow}^\dagger c_{l,\uparrow}|P\rangle = \frac{1}{L}, \tag{9}$$

$$\langle P|c_{l+1,\uparrow}^\dagger c_{l,\uparrow}|P\rangle = \langle P|c_{l-1,\uparrow}^\dagger c_{l,\uparrow}|P\rangle^* = \frac{-\sin(2\theta(\pi))}{L\sqrt{2}} e^{\mathrm{i}\pi/2}, \tag{10}$$

$$\langle P|c_{l+2,\uparrow}^\dagger c_{l,\uparrow}|P\rangle = \langle P|c_{l-2,\uparrow}^\dagger c_{l,\uparrow}|P\rangle = \frac{-\sin^2(\theta(\pi))}{2L}, \tag{11}$$

$$\tag{12}$$

and other correlations are zero. After normalizing:

$$n_\uparrow^{(P)}(k) = \frac{1}{2\pi}\left[1 - \sqrt{2}\sin(2\theta(\pi))\sin(k/2) - \sin^2\theta(\pi)\cos(2k)\right] \tag{13}$$

with $\theta(\pi) = \arctan\left[\chi + \sqrt{\chi^2+1}\right]$, with $\chi = \frac{\tilde{U}}{2\sqrt{2}\delta J_1}$. For the $\downarrow$ component the expression is identical. This expression is in excellent agreement with the blurred momentum distribution that is found in our numerics in the MC phase (Fig. 3(c) of the main text) in addition to the partially-depleted slab-like Fermi sea.

II. DERIVATION OF THE EFFECTIVE MODEL VIA MAGNUS EXPANSION

For the simplified case of a time periodic Hamiltonian, i.e. assuming that the frequencies $\Delta + U$ and Δ are integer multiples of $\omega \equiv \Delta - U$, we may obtain the same effective Hamiltonian of Eqs. (3) and (4) of the main text employing a formal Magnus expansion [1–4] or Floquet analysis [5]. Following the presentation of Ref. [4] we may express the effective Hamiltonian as a series in $1/\omega$ as $\mathcal{H}_{eff} = \mathcal{H}^{(0)} + \mathcal{H}^{(1)}_{ME} + \mathcal{O}\left(\frac{1}{\omega^2}\right)$. The lowest order term

$$\mathcal{H}^{(0)} = \frac{1}{T}\int_0^T dt_1 \mathcal{H}(t_1) \tag{14}$$

provides Eq. (3) of the main text. The first order correction in $\frac{1}{\omega}$ may be expressed as [1]

$$\mathcal{H}^{(1)}_{ME} = \frac{-\mathrm{i}}{2T}\int_0^T dt_2 \int_0^{t_2} dt_1 [\mathcal{H}(t_2), \mathcal{H}(t_1)]. \tag{15}$$

If the time periodic Hamiltonian is given by a Fourier series $\mathcal{H}(t) = \mathcal{H}_0 + \sum V^{(k)} \mathrm{e}^{ik\omega t}$, then

$$\mathcal{H}^{(1)}_{ME} = \frac{1}{\omega}\sum_k \frac{1}{k}\left([V^{(k)}, V^{(-k)}] - [V^{(k)}, \mathcal{H}_0] + [V^{(-k)}, \mathcal{H}_0]\right). \tag{16}$$

In Eq. (2) of the main text we expand the exponential term $\mathrm{e}^{\pm \mathrm{i}tUn_{j\sigma}} = 1 + (\mathrm{e}^{\pm \mathrm{i}tU} - 1)n_{j\sigma}$. Then

$$\tilde{\mathcal{H}}(t) = (J_0 + \delta J(t))\left(\mathrm{e}^{\mathrm{i}t[\Delta - U]}\bar{V}^{(1)} + \mathrm{e}^{\mathrm{i}t\Delta}\bar{V}^{(2)} + \mathrm{e}^{\mathrm{i}t[\Delta+U]}\bar{V}^{(3)} + \mathrm{H.c.}\right) \tag{17}$$

with

$$\bar{V}^{(1)} = \sum_{j,\sigma} d^\dagger_{j,\sigma} c_{j+1,\sigma} - d^\dagger_{j,\sigma} d_{j+1,\sigma}\,,$$
$$\bar{V}^{(2)} = \sum_{j,\sigma} \left(d^\dagger_{j,\sigma} - c_{j,\sigma}\right)\left(d^\dagger_{j+1,\sigma} - c_{j+1,\sigma}\right)\,,$$
$$\bar{V}^{(3)} = \sum_{j,\sigma} c^\dagger_{j,\sigma} d_{j+1,\sigma} - d^\dagger_{j,\sigma} d_{j+1,\sigma}\,. \tag{18}$$

where we employ the correlated annihilation operator $d_{j,\sigma} \equiv n_{j,\bar{\sigma}} c_{j,\sigma}$. Neglecting terms of order $J_0 \delta J$ and δJ^2 we may write

$$\mathcal{H}^{(1)}_{ME} = \frac{J_0^2}{\Delta - U}\left[\bar{V}^{(1)}, \bar{V}^{(1)\dagger}\right] + \frac{J_0^2}{\Delta}\left[\bar{V}^{(2)}, \bar{V}^{(2)\dagger}\right] + \frac{J_0^2}{\Delta + U}\left[\bar{V}^{(3)}, \bar{V}^{(3)\dagger}\right] + \mathcal{O}\left(\delta J\right), \tag{19}$$

which after some algebra yields Eq. (4) of the main text.

[1] M. M. Maricq, Phys. Rev. B **25**, 6622 (1982).
[2] G. Jotzu *et al.*, Nature **515**, 237 (2014).
[3] N. Goldman and J. Dalibard, Phys. Rev. X **4**, 031027 (2014).
[4] M. Aidelsburger *et al.*, Nature Physics **11**, 162 (2015).
[5] C. Sträter, S. C. Srivastava and A. Eckardt, arXiv:1602.08384 (2016).